

ELECTRON TRIPLETS AND PAIRS  
OBSERVED IN A STREAMER CHAMBER\*

D. Benaksas<sup>†</sup> and R. Morrison<sup>††</sup>

High Energy Physics Laboratory  
Stanford University, Stanford, California

ABSTRACT

We have studied electron pair photoproduction in the field of the nucleus and in the field of the atomic electrons of neon. A streamer chamber which in many ways behaves as a bubble chamber has been used for this experiment. The recoiling electron is observed and its momentum deduced from its curvature in a magnetic field. Most results agree with theory, in particular the triplet cross section, although the momentum distribution of the recoiling electron seems to fall more rapidly than expected.

We also report the results of several tests that have been made in order to determine the usefulness of streamer chambers with incident electron and photon beams.

(To be submitted to The Physical Review)

---

\*Work supported by the U. S. Atomic Energy Commission

<sup>†</sup>Now at Laboratoire de l'Accélérateur Linéaire, Orsay, France

<sup>††</sup>Now at Universidad Nacional de Ingenieria, Lima, Peru

## I. INTRODUCTION

Electron pair and triplet production in the field of a charged particle are processes entirely described by quantum electrodynamics; however, many approximations are necessary for a satisfactory solution of these problems. The Bethe-Heitler<sup>1</sup> formula, using the Fermi-Thomas model for screening, describes well the total pair production cross section; one has to subtract only the coulomb correction<sup>2</sup> from the Born approximations which, in the case of neon, is of order 1.3%. In the triplet case the recoiling electron changes the kinematics and gives rise to a retardation effect; in addition, the presence of two identical electrons gives rise to exchange effects. Finally one has to consider the  $\gamma$ -e interaction between the photon and the electron in whose field the pair has been created. It has been shown that the  $\gamma$ -e interaction and exchange effects are small at high energy and have an opposite effect on the total cross section, thus partially canceling; neglecting them therefore leads to a small error in the total cross section. However, these effects can be important in the high momentum transfer region, as is found in this experiment. The retardation effect has been taken into account by Borsellino<sup>4</sup> who neglected screening, while Wheeler and Lamb<sup>5</sup> calculated the triplet cross section with screening taken properly into account but with the retardation effect neglected. It has been suggested<sup>6</sup> that the best approximation for the triplet cross section is given by the following expression:

$$\sigma_t = \sigma_{\text{Wheeler-Lamb}} - \left[ \sigma_{\text{Bethe-Heitler}}^{\text{(unscreened, } Z=1\text{)}} - \sigma_{\text{Borsellino}}^{\text{(}} Z=1 \text{)} \right]$$

The momentum distribution of the recoil electron has been extracted by Suh and Bethe<sup>7</sup> from Borsellino's calculation.

Triplet photoproduction was first directly measured by Hart et al.<sup>8</sup> in a cloud chamber, later by Gates et al.<sup>9</sup> in a bubble chamber. Most of the results obtained in these experiments agree well with the theory. So far no direct triplet experiment has been performed on nuclei heavier than hydrogen, primarily

because of the difficulty in detecting electrons of low energy. Also the ratio of triplet cross section to pair cross section goes as  $1/Z$ ; this ratio is roughly 0.1 for neon and 1 for hydrogen. Therefore, one has to take many more pictures with neon than with hydrogen to observe the same number of triplets. Although the production process does not depend strongly on the  $Z$  of the material, the screening of the atomic electrons and the binding forces may change the behavior of the process. A streamer chamber is a suitable instrument for such a study, the target being the neon which fills the chamber. The gas is a mixture of neon (90%) and helium (10%); about 0.5% of events originate from helium. Momenta are measured using the curvature and dip angle in a weak magnetic field (2 Kg), but between 0.2 MeV/c and 0.4 MeV/c we have used in many cases the range energy method. Photons from the bremsstrahlung spectrum were tagged in order to reduce the data taking to the photon energy band 600 - 800 MeV; the tagging was also helpful in reducing substantially the number of pictures due to background.

## II. APPARATUS

Figure 1 shows the general arrangement of this experiment. The electron beam, after passing through the radiator, was deflected by a magnet towards some shielding blocks. The electrons that emitted radiation in the energy range 600 - 800 MeV were deflected towards a group of 3 tagging counters with a common backing counter in coincidence. Beam intensity and radiator thickness were chosen such that each front counter counted about one electron per pulse ( $1 \mu s$ , 60 cps). These tagging counters were used as a monitor for the photon beam. A small amount of hardener (0.2 radiation length of Be) in the X-ray beam was necessary to cut down substantially the number of low energy Compton electrons

which otherwise might be mistakenly regarded as recoil electrons when produced near an electron pair vertex. A collimator immediately after the hardener prevented the large angle photons from reaching the spark chamber walls.

#### A. Streamer Chamber

Streamer chambers have been developed<sup>10-13</sup> some years ago, but as yet have rarely been used in physics. The techniques of construction and the operation of very large streamer chambers have been discussed in a detailed paper.<sup>14</sup> We constructed a small streamer chamber to be used in a magnet in order to perform a series of tests using the electron beam at the Stanford Mark III accelerator. This chamber is  $38 \times 30 \times 13 \text{ cm}^3$  with walls made of 1.2 cm lucite. Two perpendicular sets of wires stretched on an aluminum frame constitute a transparent high voltage plate, allowing photography from above the chamber. The wires are isolated from the neon gas by a 0.6-cm lucite plate, assuring at the same time a gas seal. The ground plate is made from 0.6 cm thick aluminum. Both plates have rounded corners to decrease corona effects and extend 2.5 cm outside the chamber in order to make the electric field uniform and avoid breakdowns in the chamber. A slow flow of Ne-He mixture gas is maintained continuously through small holes in the walls.

#### B. Driving System

To be operating in the streamer mode, the chamber needs a very short pulse, 8 to 10 ns wide and of 15 to 20 kV/cm. A classical Marx generator (10 stages) with a power supply ( $\pm 30 \text{ kV}$ ) delivers 220-kV pulses with a tail of about 100 ns. When directly applied on the chamber, such a pulse produces a discharge between the plates along the track of an ionizing particle. To shape the pulse, we use only a shorting gap operating under 40 pounds pressure of SF<sub>6</sub>, following the Marx. Although the chamber is not long enough to behave as a

transmission line, it was found that the best pulse is obtained when the chamber is terminated by 250 ohms. This arrangement, shown in Fig. 2, is far from being sophisticated; nevertheless such a system is able to drive small size chambers such as the one used in this experiment. In Fig. 3 we show a typical pulse applied to the chamber. For chambers of medium size, a capacity and a series gap may be inserted between the chamber and the Marx generator; for very large chambers, a Blumlein seems the best solution.

### C. Operation of the Chamber

By shorting the pulse to about 10 ns, one can stop the development of the avalanches initiated after the passage of an ionizing particle so that, instead of a spark connecting the plates, one has a series of streamers directed along the electric field. About three streamers per cm are produced on the average in the gas and their length may vary from a few mm to a few cm depending upon the voltage and the width of the pulse applied. We usually keep the voltage constant and change the width by varying the pressure in the shorting gap in a manner such that the streamer's length is adjusted between 4 to 10 mm. Below 4 mm the streamers look very faint when seen by the camera from the side view through a mirror but are sufficiently bright when seen directly from the top. A part of the top pole of the magnet has been removed to allow photography. Kodak 2475 film was used with an f/1.4 lens in this experiment. Figures 4 and 5 show typical events obtained in the small chamber. Vertices are perfectly visible in the volume of the chamber as are the trajectories of all ionizing particles independent of their angle. However, there is an anisotropy in the brightness of the tracks, the tracks crossing the plates being brighter than those parallel to the plates. The chamber may be triggered on specific events just as any conventional spark chamber although the sensitive time of the streamer chamber is much longer. This is not a disadvantage at Mark III where the beam pulse length

is  $1 \mu\text{sec}$ . We can use either the neon of the chamber as target, as done in this experiment, or an internal target. A thin sulphur plate has been used, for example, to study the high energy end of the bremsstrahlung spectrum; the non-uniformity of electric field does not appreciably disturb the formation of streamers nor the apparent position of the trajectories. In this bremsstrahlung experiment the incident and the final electrons were observed and their momentum measured while the emitted photon was detected in a shower counter. In another test we inserted a cylinder of mylar (2.5 cm in diameter) containing hydrogen in the mid-plane of the chamber and passed an electron beam through it. The streamers did not form in hydrogen and therefore one could not see the vertex which could be reconstructed from the trajectories of final charged particles visible outside the cylinder. Up to 200 quanta per pulse can be injected in such a chamber with less than one electron pair visible in the chamber. A system, similar in design but physically much larger, will be used for photoproduction studies.<sup>15</sup> We have attempted to use electrons in a similar manner in order to do electroproduction studies. We found that the number of electrons which can be injected in the hydrogen cylinder without producing a large background in the chamber is limited to about 3000 per pulse. This background is mainly low energy electrons which spiral above and below the cylinder when a magnetic field is applied.

### III. PROCEDURE AND MEASUREMENTS

In this experiment, a signal in any one of the tagging counters corresponds to the emission of a photon in the energy range 600 - 800 MeV. If such a photon converts in the chamber, one member at least of the electron pair produced has its energy greater than 300 MeV. The magnetic field in the chamber and the

position of the trigger counters were adjusted such that these counters detected electrons (and positrons) of energies ranging between 300 MeV and 800 MeV. The chamber was fired when a signal from either the left or right trigger counters was in coincidence with a signal from any of the 3 tagging counters; the tagging counter which gives the coincidence was recorded in the picture by an appropriate light. Pictures were taken by one camera only which viewed the top view directly, and the side view through a mirror. Events were measured with a fitting program written for us by D. Fries for the case of an inhomogenous field. All tracks were fitted to a common vertex and the momenta and angles were calculated. The typical resolution for small angles is 5 milliradians while the momentum is calculated within 5 to 10%. In some cases the side view was not clearly visible on the picture, mainly because the streamers happened to be too long due to variations in the electric pulse length. In these cases, only the top view was measured and gave information on projected values only.

#### IV. RESULTS

##### A. Recoil Momentum Distribution

The typical recoil momentum, in electron pair production, is of order of the electron mass. When the recoil particle is an electron, the kinetic energy is large enough to enable us to observe it in the streamer chamber. For momenta greater than 0.4 MeV/c, all events are measured using the curvature of the recoil electron and its dip angle. For momenta smaller than 0.4 MeV/c, we could use the same method for some events, while for others the range energy relation was used. The differential recoil momentum distribution is shown in Fig. 6. Experimental points are shown with the statistical error and with the energy band resolution; the solid points represent events where momenta were measured using curvature and dip angle, the square points correspond to events measured

mostly by the range-energy method. The minimum detectable momentum seems to be 0.2 MeV/c or 36 keV in our streamer chamber, the limitation being due to streamer length; the first point below 0.2 MeV/c is thus not expected to be correct. Nine events were found with momentum greater than 48 MeV/c; the highest recoil momentum was 130 MeV/c. The solid curve is that calculated by Suh and Bethe; as discussed above, it is expected to be correct for momentum not too small, since the screening, which has been neglected, is important for small momenta only. The experimental points are normalized to fit the theoretical curve at  $q = 1.05$  MeV/c. As far as the general behavior of the distribution is concerned, it seems to have a steeper slope than expected, the experimental points lying below the theoretical curve for high momentum transfer. The same effect has been seen by Gates, *et al.*, in hydrogen.

### B. Evaluation of the Triplet Cross Section

A direct measurement of the total triplet cross section is not possible because the minimum recoil momentum is much lower than our limit of momentum measurement. One can expect, however, a good estimation of the triplet cross section  $\sigma_t(q_o)$  for recoil momentum greater than some value  $q_o$ . One has to measure first the total number  $N$  of pairs produced in the chamber, whether or not we observe a recoil electron.  $N$  is then proportional to  $\sigma_p + \sigma_t$ , the sum of the total cross sections for pair and triplet production. Then we measure the number  $N(q_o)$  of triplets which have a recoil momentum greater than  $q_o$ ;  $N(q_o)$  is proportional to  $\sigma_t(q_o)$ . This gives:

$$\sigma_t(q_o) = \frac{N(q_o)}{N} (\sigma_t + \sigma_p)$$

Almost all systematic errors cancel in the experimental ratio  $N(q_o)/N$ . Table 1 compares  $\sigma_t(q_o)$  obtained from Suh and Bethe calculations and deduced from this

experiment. We have used  $E_\gamma = 700$  MeV in the calculations, which has been taken as the mean value for the photon energy-band 600 - 800 MeV. Note that  $\sigma_t(q_o)$  depends only slightly on the photon energy when this energy is greater than 100 MeV.

TABLE I

$q_o$ (MeV/c)	$\sigma_t(q_o)$ theory (millibarns)	$\sigma_t(q_o)$ experimental (millibarns)	$\frac{\sigma_t(q_o)}{\sigma_t(q_o)}$ exp. $\frac{\sigma_t(q_o)}{\sigma_t(q_o)}$ th.	$\frac{\sigma_t(q_o)}{\sigma_t}$
0.5	20.2	$21.0 \pm 1.10$	$1.04 \pm 0.05$	0.235
1	12.1	$12.2 \pm 0.76$	$1.01 \pm 0.06$	0.147
2	6.94	$6.2 \pm 0.52$	$0.91 \pm 0.08$	0.0845
5	3.12	$2.74 \pm 0.37$	$0.88 \pm 0.12$	0.038

The errors assigned are partly statistical and partly due to possible errors in the determination of  $q_o$ . The last column of Table I shows that we observe 23.5% of the triplet cross section when  $q_o = 0.5$  MeV/c, while we observe only 3.8% when  $q_o = 5$  MeV/c. We have not calculated the results for  $q_o < 0.5$  MeV/c because momentum measurements are inaccurate in this region as explained in the preceding paragraph. Column 4 shows a good agreement between experiment and theory for low momentum transfer; however, there is some slight evidence that  $\sigma_t(q_o)$  experimental drops faster than expected. The possible discrepancy with theory, between  $q_o = 0.5$  and  $q_o = 5$  MeV/c is about 16% and could be attributed to exchange effects since these effects arise mainly in large momentum transfer collisions where all three electrons have high energy; in this case, there is a reduction in phase space which produces a reduction in the cross section. One can notice that even a large discrepancy observed in the high momentum region does not greatly affect the total cross section, since the main contribution comes from the low momentum

region. Exchange terms as well as  $\gamma$ -e interaction terms are clearly involved in the case where the two electrons have high energy while the positron has low energy; the contribution of these terms calculated by Votruba<sup>16</sup> is of order  $\frac{2}{3} \frac{m}{k} \ln \frac{k}{m} \simeq 3 \cdot 10^{-3}$  relative to the leading term. The same calculation performed for the case where all particles have high momentum leads to a contribution of order 0.02. Thus, as far as the high momentum transfer region is concerned, exchange and  $\gamma$ -e interaction will contribute approximately  $3 \cdot 10^{-3}/0.02$  or 15%. This order of correction is consistent with the discrepancy observed in the measurement of the cross section for high momentum transfer; in fact, the  $\gamma$ -e interaction is smaller than the exchange effects by a factor  $\ln(k)$  or 6.7, as discussed in Ref. 3. Therefore, one can assume that exchange effects are responsible for the main discrepancy.

### C. Angular Distribution of the Recoil Electrons

The angular distribution  $d\Phi/d\theta$ , where  $\theta$  is the angle between the recoil electron and the direction of the incident photon, is given in Fig. 7a. The overall data presents a large peak which extends from 0 to  $90^\circ$ , with a maximum around  $55^\circ$ . In fact, the angular distribution is strongly correlated with the momentum distribution; large angles correspond to low momentum transfer, and small angles to high momentum transfer. In the same figure, we give the distribution of the events for which the momentum is greater than 1 MeV/c and also for the case where the momentum lies between 0.4 and 1 MeV/c. Their common part, centered around  $55^\circ$ , corresponds to a momentum of about 1 MeV/c. One can notice that with low momentum electrons, the probability of multiple scattering is very large, therefore leading, for some events, to recoil angles greater than  $90^\circ$ . The extraction of the angular distribution from either the Borsellino or Votruba calculations is very complicated;

therefore, there is no theoretical curve to compare our results with. However, simple kinematic considerations lead to the approximate relation between the momentum and the angle of the recoil electron:  $q \simeq 2m \cos \theta / \sin^2 \theta - \alpha / 2k \cos \theta$ ;  $\alpha = p_+ p_- \omega^2$  where  $p_+$  and  $p_-$  are the positron and the electron momenta, and  $\omega$  is their opening angle; the second term of the above relation is very small,  $\alpha$  being typically of order 4 m. Fig. 7b shows the diagram of the momentum  $q$  versus  $\cos \theta / \sin^2 \theta$ . The events represented by the points group effectively around the line  $q = \cos \theta / \sin^2 \theta$  ( $2m \simeq 1$ ); in Fig. 7c, we show the angular distribution plotted versus  $\cos \theta / \sin^2 \theta$  instead of  $\theta$ ; it has the same behavior as the momentum distribution of Fig. 6. The first 3 points in Fig. 7c are not expected to be correct, because the recoil angle could not be measured for all low momentum events.

#### D. Energy Sharing Distribution

The energy of both electrons of the pair was measured. The fraction of the pair energy, carried away by the positron, is expressed by  $f \simeq E_+ / (E_+ + E_-)$ . The  $f$  distribution is presented in Fig. 8. Because the magnetic field was low, we used only a small part of the data, i.e., the pairs which occurred in the first two inches of the chamber; for these events, the electron's trajectory length is about 32 cm, which gives an accuracy in the momentum measurement of order 5%. Only about 100 triplets were found in this region, which was not enough to study their energy distribution; therefore, we used only the pairs produced in the nuclear field. The solid curve is that of Bethe and Heitler, calculated for  $E_\gamma = 700$  MeV and  $Z = 10$ . The experimental distribution presents the general behavior predicted by the theory, with a symmetry around  $f = 0.5$ . However, the dip and the maxima seem more accentuated. An uneven energy sharing seems to be preferred.

### E. Conclusions

The first conclusion to be drawn from this experiment concerns the streamer track chamber. It has been shown that it possesses many qualities useful for high energy experiments. Because it can be triggered and because it shows isotropy similar to a bubble chamber, one hopes that this new tool will be widely and successfully used in the future. It enabled us to study triplet photoproduction in a very satisfactory way in a material heavier than hydrogen.

The measured triplet cross section was found to be consistent with calculations for the electron recoil momentum  $q_0$  near 1 MeV/c but might indicate a slight divergence when  $q_0$  increases, as is most clearly visible in the momentum distribution. The discrepancy observed is of the proper sign to be attributed to exchange effects which arise mostly at high momentum transfer. Further investigations of the high momentum region seem necessary to provide a better understanding of the recoil momentum and angular distributions in pair production in the field of the electron.

### Acknowledgements

We wish to thank R. Mozley for his constant support of this work, and A. Odian, F. Villa and D. Yount for their help in solving streamer chamber problems. We are grateful to D. Drickey for the active part he took in all phases of the experimental preparation and in the data taking, and to D. Fries for his help in the analysis problems.

### References

1. H. A. Bethe and W. Heitler, Proc. Roy. Soc. (London) A146, 83 (1934).
2. H. Davies, H. A. Bethe, and L. C. Maximon, Phys. Rev. 93, 788 (1953).
3. J. Joseph and F. Rohrlich, Revs. Modern Phys. 30, 354 (1958).
4. A. Borsellino, Helv. Phys. Acta 20, 136 (1947); Nuovo Cimento 4, 112 (1947).
5. J. A. Wheeler and W. E. Lamb, Phys. Rev. 55, 858 (1939).
6. H. A. Bethe and A. Ashkin in Experimental Nuclear Physics, edited by E. Segrè, (1953), Vol. I, Part II, p. 263.
7. K. S. Suh and H. A. Bethe, Phys. Rev. 115, 672 (1959).
8. E. L. Hart, G. Cocconi, V. T. Cocconi, and J. M. Sellen, Phys. Rev. 115, 678 (1959).
9. Duane C. Gates, Robert W. Kenney, and William P. Swanson, Phys. Rev. 125, 1310 (1962).
10. S. Fukui and S. Miyamoto, Nuovo Cimento 11, 113 (1959).
11. A. A. Borisow, B. A. Dolgoshein, B. I. Luchkov, L. V. Reshtin, and V. I. Ushakov, Pribori i Tekhn., Exp. 1, 49 (1962).
12. G. E. Chikovani, V. A. Mikhailov, and V. N. Roinishoili, Physics Letters 6, 254 (1963).
13. V. A. Mikhailov, V. N. Roinishoili and G. E. Chikovani, JEPT 18, 561 (1964).
14. Streamer Chamber Development: F. Bulos, A. Odian, F. Villa, and D. Yount (to be published).
15. I. Derado, D. Drickey, D. Fries, R. Mozley, A. Odian, F. Villa, and D. Yount, Experimental Proposal for a Study of High Energy Photoproduction at SLAC
16. V. Votruba, Bull. Intern. Acad. Tcheque Sci. 49, 19 (1948).

### List of Figures

1. Experimental setup.
2. Streamer chamber driving system.
3. General shape of the electric pulse.
4. Typical triplet event; the side view, showing the streamers in the electric field direction, is represented in the right side of the picture; notice that for large dip angle the streamers join together to form a continuous track. This is clearly visible for the recoil electron.
5. Positrons passing through a streamer chamber set up in a magnetic field. One Compton electron may also be seen.
6. Recoil momentum distribution. The solid curve is that of Suh and Bethe. The full points have been measured using the curvature and the dip angle; the square points have been measured partly by the same technique and partly by range. Experimental points are normalized to fit the curve at  $q = 1.05 \text{ MeV}/c$ .
- 7a. Angular distribution of the recoil electrons. The curves represent only a smooth fit to the data.
- 7b.  $\cos \theta / \sin^2 \theta$  versus the momentum  $q$  where  $\theta$  and  $q$  are the angle and the momentum of the recoil electron.
- 7c. Angular distribution of the recoil electron; the abscissa is  $\cos \theta / \sin^2 \theta$ . The first 3 points are not expected to be correct (see text).
8. Energy sharing distribution for pairs produced in the field of the nucleus. The solid curve is that of Bethe and Heitler.

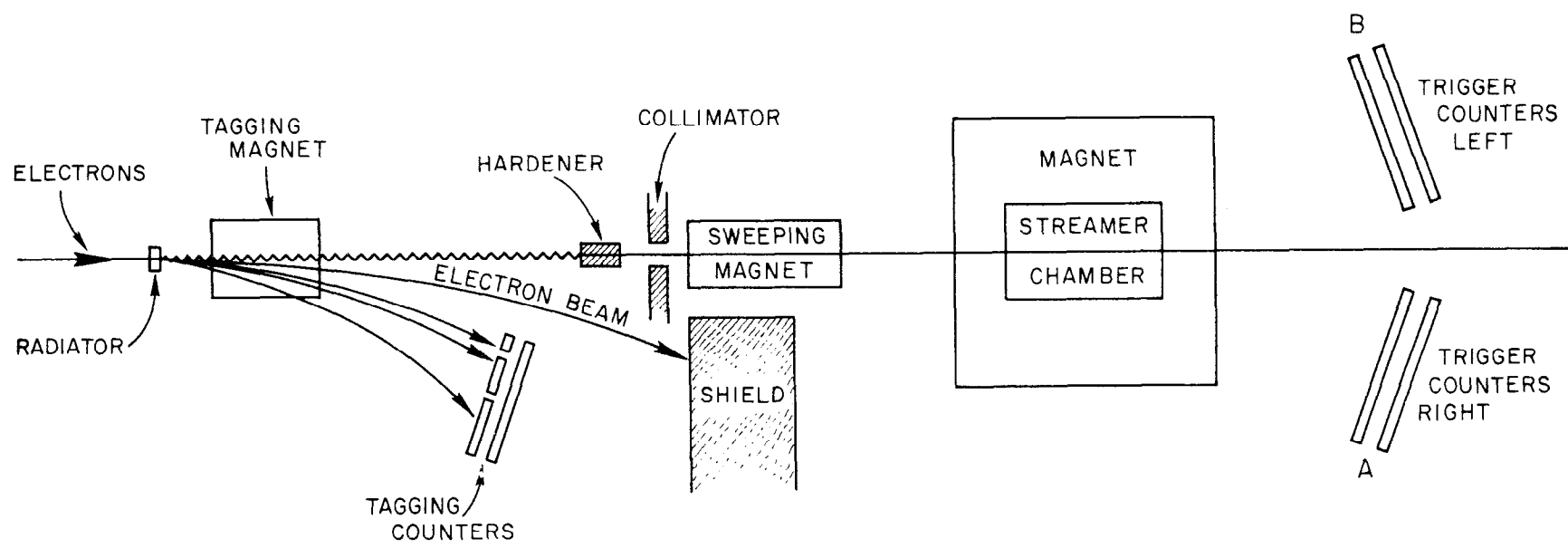
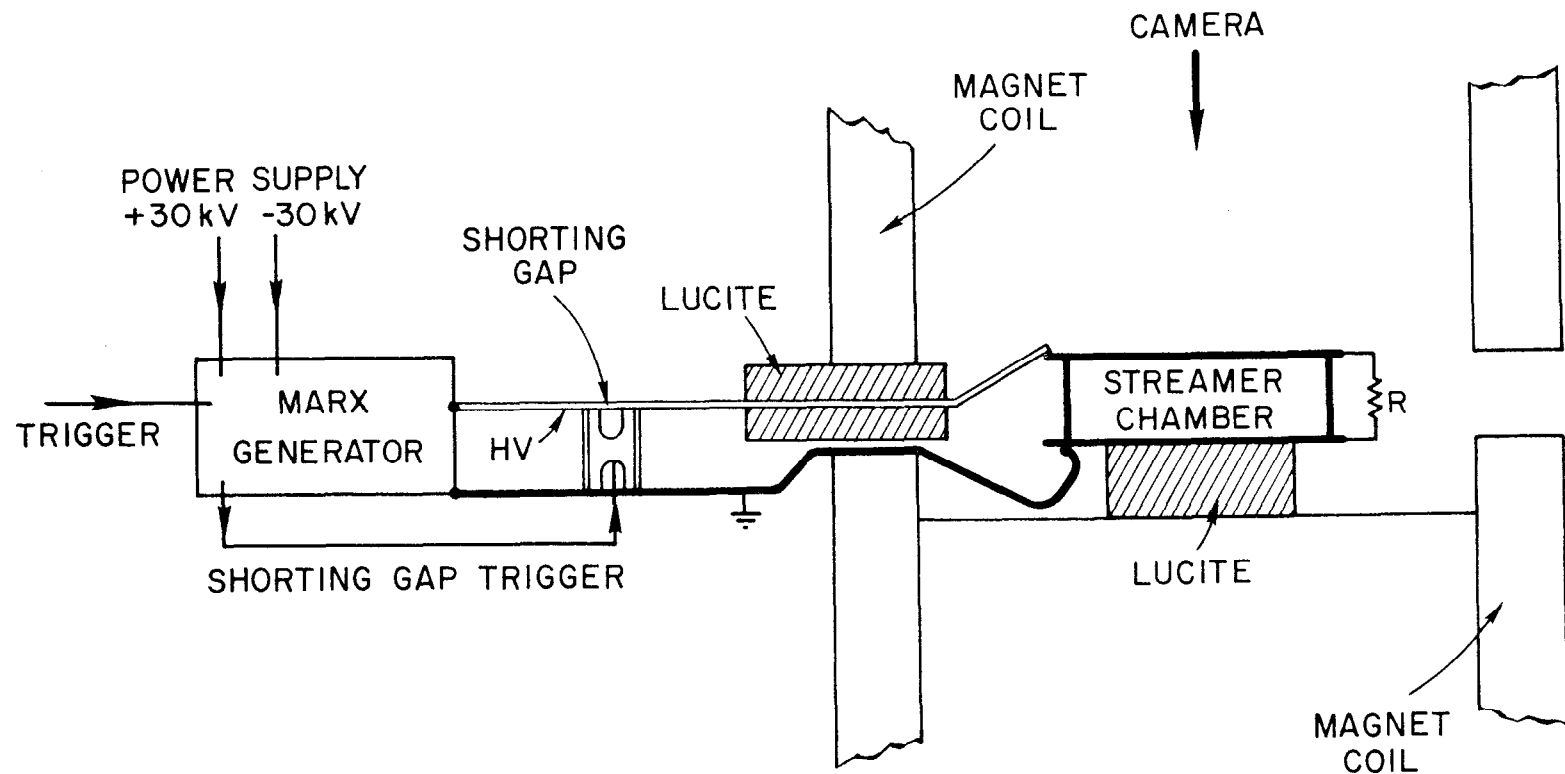


FIG. 1



698A2

Fig. 2

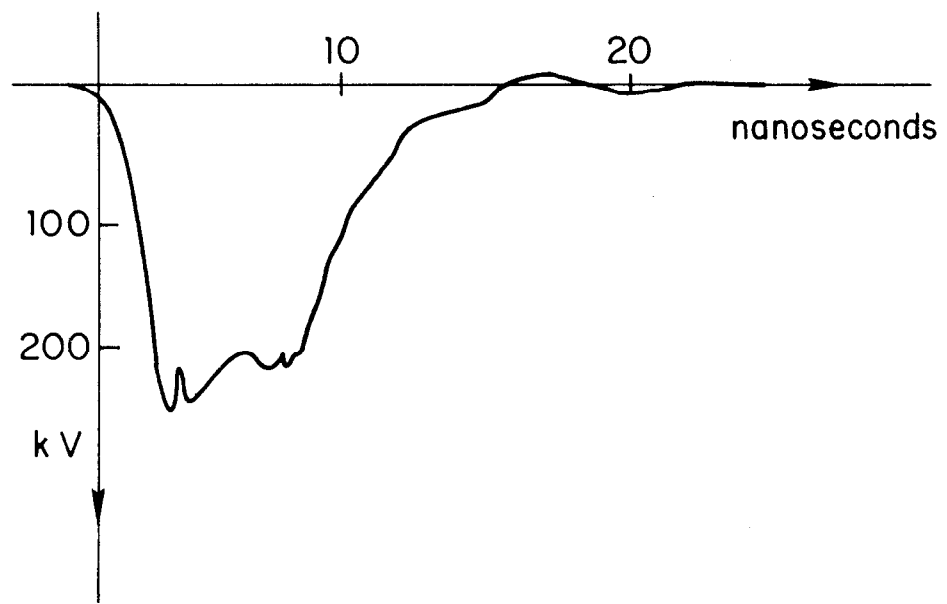


Fig. 3

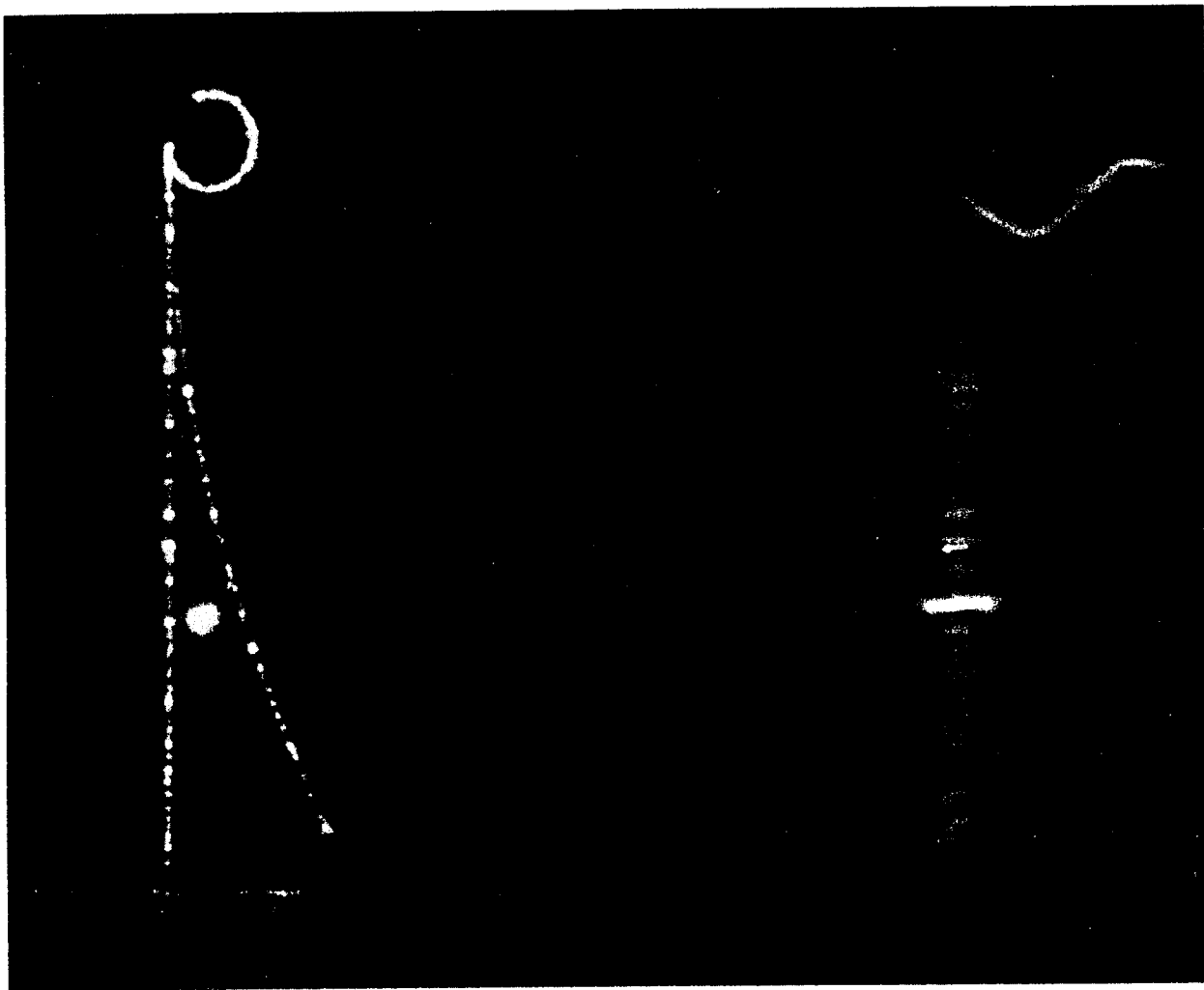


FIG. 4



Fig. 5

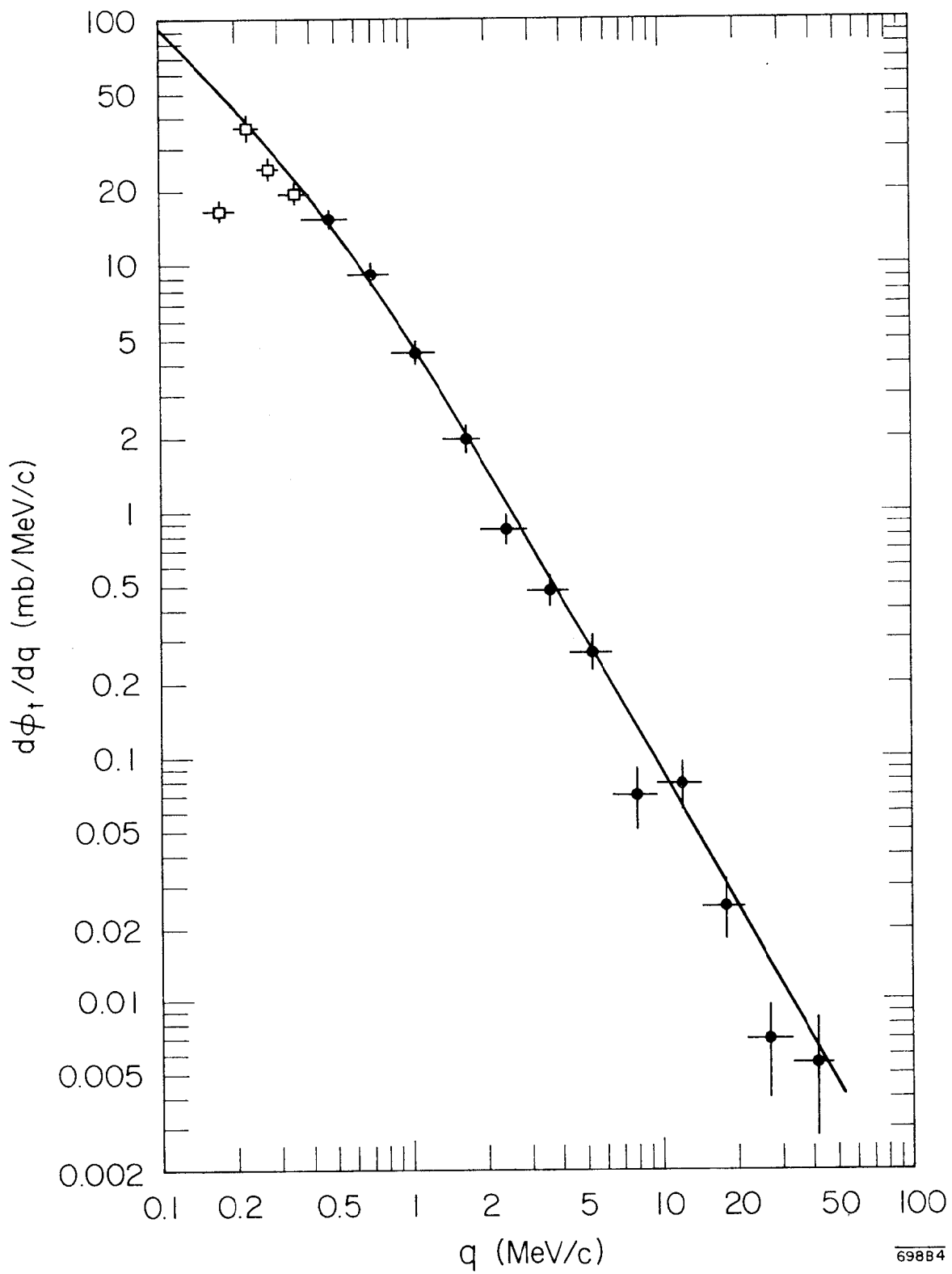


FIG. 6

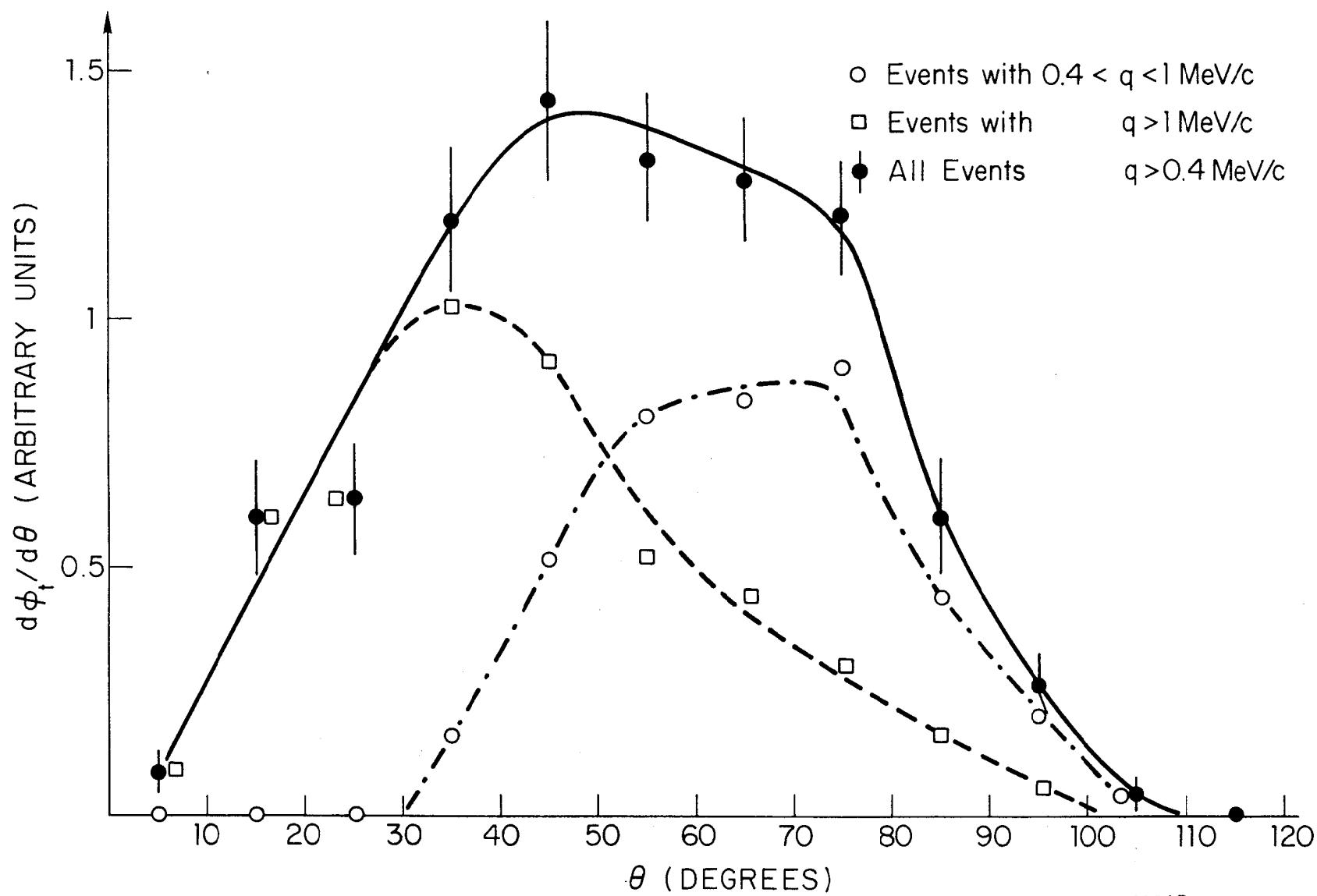


Fig. 7a

698A5

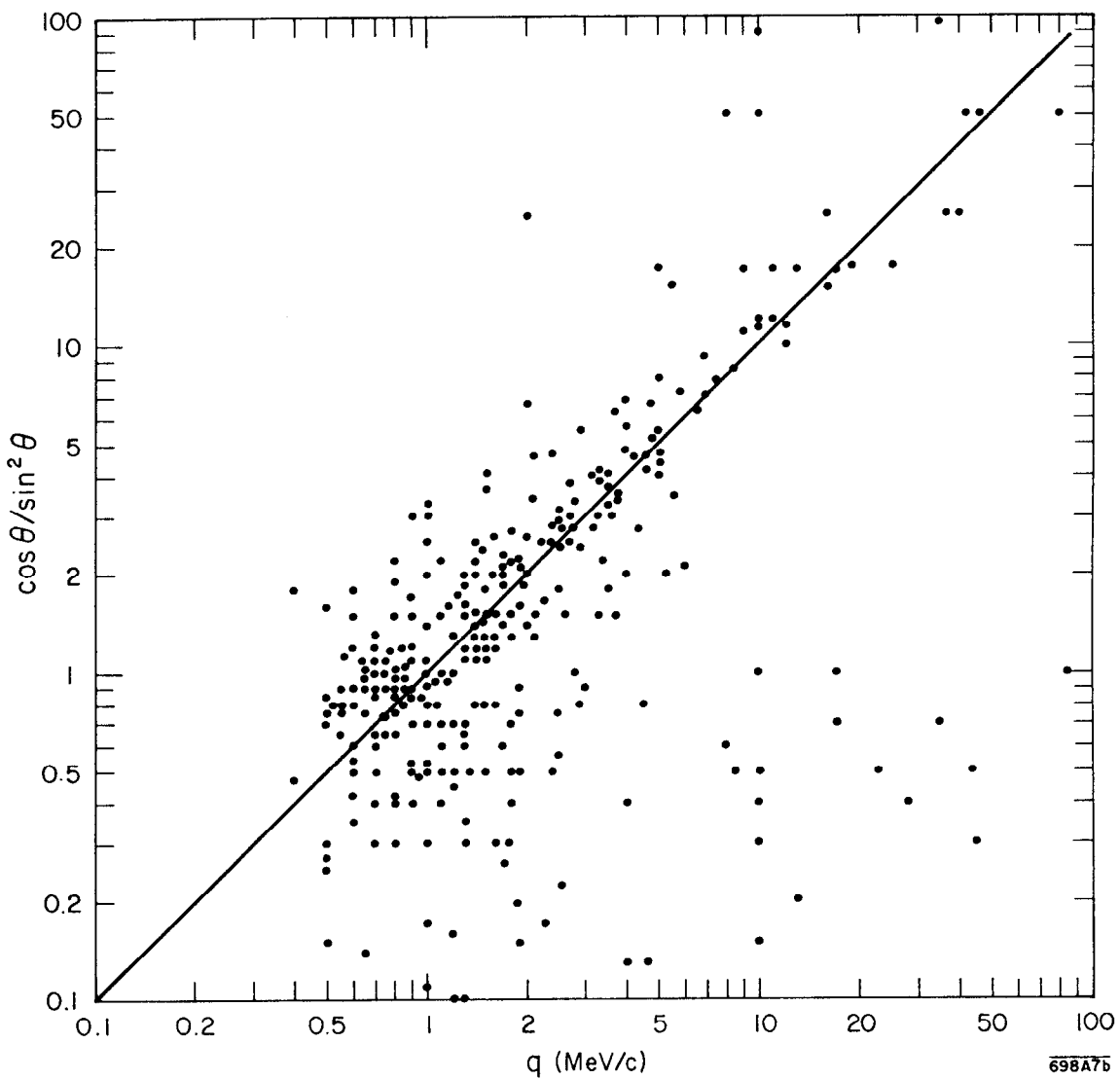


FIG. 7b

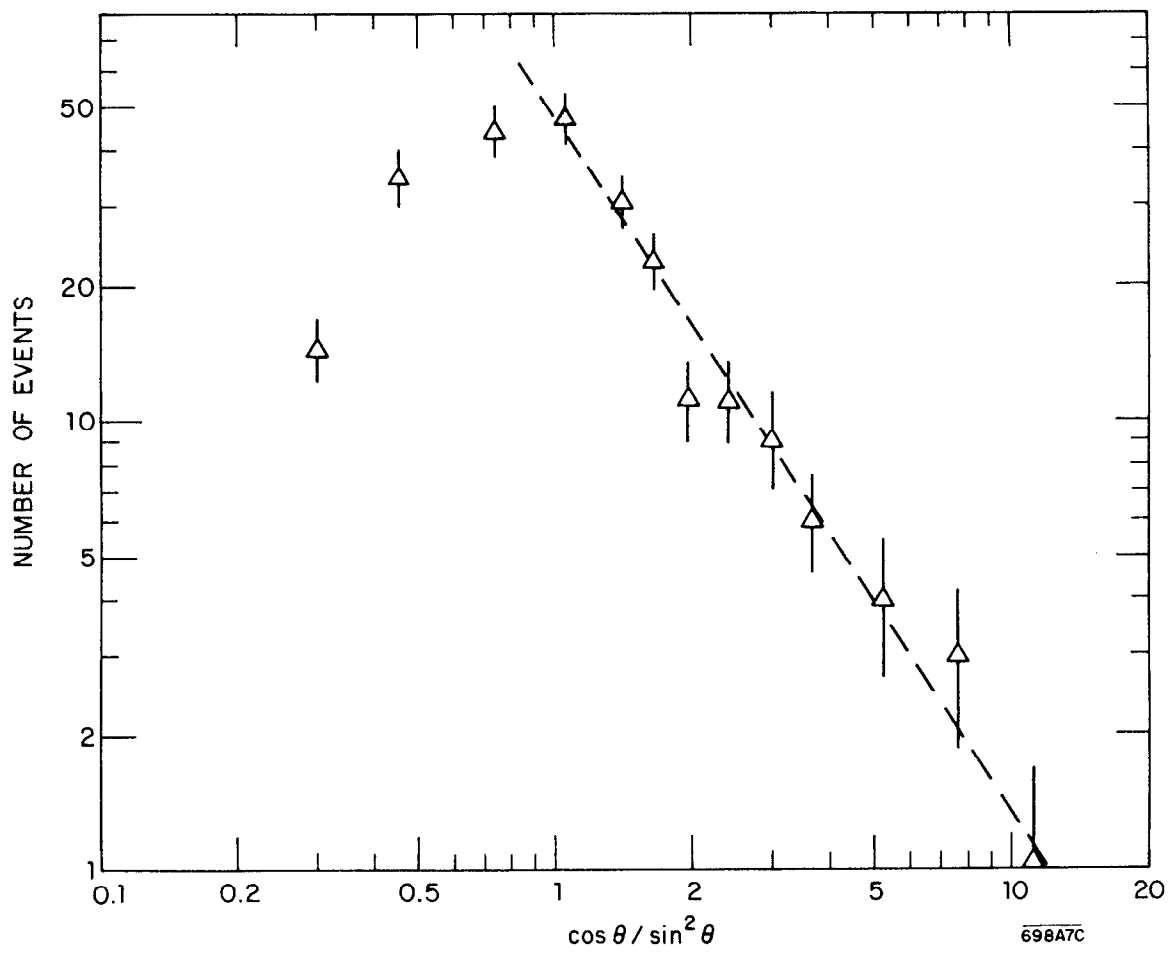


FIG. 7c

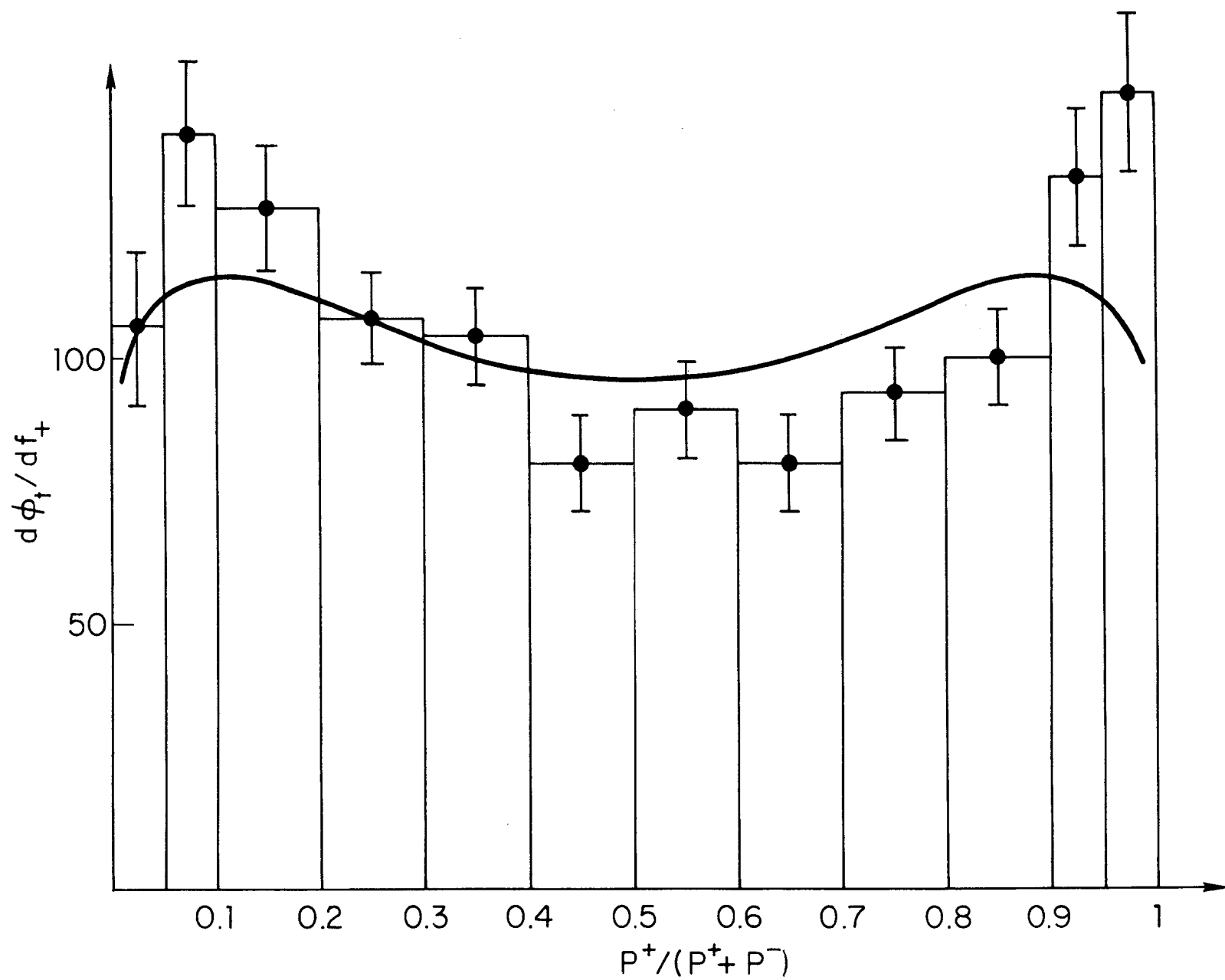


Fig. 8